ELSEVIER

Physics Letters B 526 (2002) 287–294

PHYSICS LETTERS B

www.elsevier.com/locate/npe

Coherent π^0-photoproduction from atomic nuclei

B. Krusche [a], J. Ahrens [b], R. Beck [b], S. Kamalov [c], V. Metag [d], R.O. Owens [e], H. Ströher [f]

[a] *Department of Physics and Astronomy, University of Basel, Ch-4056 Basel, Switzerland*
[b] *Institut für Kernphysik, Johannes-Gutenberg-Universität Mainz, D-55099 Mainz, Germany*
[c] *Laboratory of Theoretical Physics, JINR Dubna, Russia*
[d] *II. Physikalisches Institut, Universität Giessen, D-35392 Giessen, Germany*
[e] *Department of Physics and Astronomy, University of Glasgow, Glasgow G128QQ, UK*
[f] *Institut für Kernphysik, Forschungszentrum Jülich GmbH, 52425 Jülich, Germany*

Received 4 December 2001; received in revised form 10 December 2001; accepted 18 December 2001

Editor: J.P. Schiffer

Abstract

Differential and total cross sections for coherent π^0-photoproduction from ^{12}C, ^{40}Ca, ^{93}Nb and Pb targets have been measured throughout the region of the $\Delta(1232)$-resonance. The experiments were performed with the TAPS-detector at the Mainz accelerator MAMI. The characteristic proportionality of the cross section to the square of the atomic mass number and to the nuclear mass form factor is clearly demonstrated. The data allow for the first time detailed tests of model predictions for this reaction. The comparison of the data to model predictions shows that the Δ-nucleus interaction saturates: it is described for heavy nuclei with the same potential parameters as for ^{4}He.

1. Introduction

The study of meson photoproduction from atomic nuclei is mainly motivated by two strongly interconnected aspects namely possible medium modifications of the excited states of the nucleon and the meson–nucleus interaction. Three different reaction mechanisms can contribute for neutral mesons: coherent production where the reaction amplitudes from all nucleons add coherently and the nucleus remains in its ground state, incoherent meson production with an excited nucleus in the final state, and breakup reactions where at least one nucleon is knocked out of the nucleus. The theoretical treatment of coherent meson production involves many fewer assumptions and approximations than are needed for the description of the complicated final states from breakup reactions. For the latter so far only semiclassical calculations, e.g., in the framework of transport models [1] or mean free path Monte Carlo calculations [2] are available. In light nuclei with only a few excited states, incoherent excitations of the nucleus can be exploited as spin–isospin filters, but their treatment becomes very complicated for heavy nuclei with a high level density.

E-mail address: bernd.krusche@unibas.ch (B. Krusche).

0370-2693/02
PII: S0370-2693(01)01503-9

As long as final state interaction (FSI) of the mesons is neglected, the cross section of breakup reactions scales with the mass number of the nuclei but the differential cross section of the coherent process is proportional to the square of the mass number and the nuclear mass form factor. Due to the form factor dependence, the coherent process is negligible compared to breakup reactions at large momentum transfers. For this reason the in-medium properties of higher lying nucleon resonances were only investigated via quasifree pion or eta photoproduction (see, e.g., [3,4]). However, the situation is different for the excitation of the lowest lying nucleon resonance, the so-called Δ-resonance ($P_{33}(1232)$ in the usual notation [5]). The momenta transfered to nuclei in pion photoproduction to forward angles are so small that the coherent process is dominant for heavy nuclei. Furthermore, the elementary photoproduction of neutral pions from the nucleon is well understood in this energy region and strongly dominated by the excitation of the Δ-resonance [16].

Coherent π^0-photoproduction has been extensively treated in the framework of different models. One group of models, which mainly aim at the study of the pion–nucleus interaction and the in-medium properties of the pion, use the distorted wave impulse approximation (DWIA) (see, e.g., [6–9]). Starting from the elementary pion–nucleon amplitude this approach dynamically takes into account final state interactions (FSI) of the pion in the nuclear medium but neglects medium modifications of the resonance properties (position and widths). On the other hand the in-medium properties of the Δ-resonance have been intensively studied in the framework of the Δ-hole approach with special attention to the Δ and pion dynamics but mostly without non-resonant contributions in the elementary production process (see, e.g., [10–12]). In the case of ^{12}C Takaki et al. [13] have extended this calculations to incoherent contributions from low-lying nuclear excitations. Since the Δ-hole calculations are numerically quite involved, they have been mostly restricted to light nuclei. Carrasco et al. [14] have tried to overcome this difficulty with a local approximation of the Δ-hole model, which made calculations feasible even for lead. Prompted by the growing interest in medium modifications of hadrons and the expected availability of new, precise data, several extensions of the existing models have been discussed recently. In the framework of the DWIA approach Drechsel and coworkers [15] presented a calculation which starts from their Unitary Isobar Model for the elementary reaction [16] and includes a phenomenological parametrization of the Δ self-energy. Peters et al. [17] developed a relativistic non-local model which includes medium modifications in the production operator of the Δ-resonance. Abu-Raddad et al. [18] emphasized the ambiguities arising already from the extrapolation of the elementary amplitude off the mass shell in the relativistic impulse approximation.

On the experimental side progress was much slower. In a very early attempt Schrack et al. [19] measured unnormalized pion yield curves for light to medium mass nuclei. Since then differential and total cross sections have been measured for carbon and calcium nuclei in the threshold region [20,21] but only one attempt was made to measure the cross section throughout the Δ-resonance for carbon [22]. Only recently measurements up to much higher incident photon energies were reported for deuterium and helium nuclei [23–26].

2. Experiment and analysis

In this Letter we present the results of measurements of coherent π^0-photoproduction from ^{12}C-, ^{40}Ca-, ^{93}Nb- and Pb-targets throughout the region of the Δ-resonance. The experiments were carried out at the Glasgow tagged photon facility installed at the Mainz Microtron (MAMI) with the TAPS-detector [27,28]. Details of the experimental setup and the data analysis are summarized in [23].

The separation of the coherent and incoherent parts is only possible via their different reaction kinematics. This was done by a comparison of the cm energy $E_\pi(\gamma_1\gamma_2)$ of the pion derived from the measurement of energy and momentum of its decay photons to the energy $E_\pi(E_\gamma)$ derived from the incident photon energy E_γ under the assumption of coherent pion production [23]. The situation for heavy nuclei differs in two aspects from the deuterium case discussed in [23]. The larger nucleon binding energies and the stronger effects of Fermi motion result in a much better separation of coherent and breakup events in missing energy. On the other hand no model independent simula-

tion of the shape of the contribution from the complicated final states of non-coherent events in missing energy is possible. Therefore only the shape of the coherent contribution was simulated and compared to the data at positive values of the pion energy difference, i.e., in the region where non-coherent components can only contribute due to finite resolution effects. Contributions from breakup reactions are almost completely removed in this way but incoherent excitations to low-lying nuclear states are only incompletely suppressed. Due to the shape of the angular distributions and the A^2-dependence of the cross section of the coherent process, residual incoherent background is mainly a concern for light nuclei and large pion angles. Examples of the measured energy difference spectra ($\Delta E = E_\pi(\gamma_1\gamma_2) - E_\pi(E_\gamma)$) and the Monte Carlo simulation are shown in Fig. 1. The measured shape is almost perfectly reproduced by the simulation at low incident photon energies and small pion angles. At higher energies or larger angles non-coherent contributions become visible.

The absolute normalization of the cross sections was done as in [23]. The total overall uncertainty due to analysis cuts, target thickness and photon flux amounts to 3%. The systematic uncertainty of the simulation of the detection efficiency is estimated to be 10%.

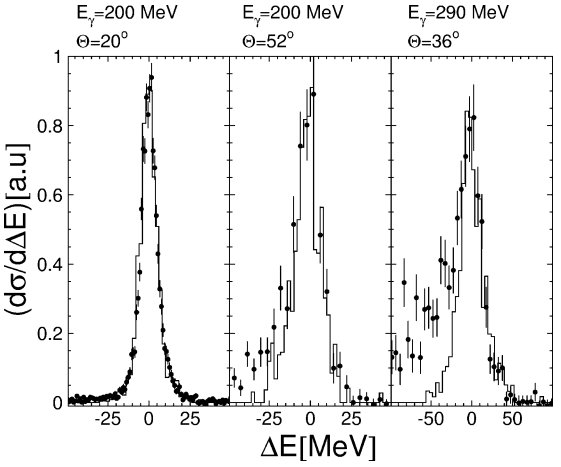

Fig. 1. Pion energy difference spectra for the reaction $\mathrm{Pb}(\gamma,\pi^0)\mathrm{X}$. Symbols with error bars represent the data, the histograms a Monte Carlo simulation of the coherent reaction $\mathrm{Pb}(\gamma,\pi^0)\mathrm{Pb}$. The energy and angle combinations correspond to the first and second maximum of the angular distribution for the incident photon energy $E_\gamma = 200$ MeV and to the second maximum at $E_\gamma = 290$ MeV (compare Fig. 4).

3. Results and discussion

The quality of the data obtained is shown in Fig. 2, where the differential cross sections averaged over photon energies from 200–290 MeV are plotted versus the momentum q_A transferred to the nucleus.

The coherent cross section for spin zero nuclei can be written in the most simple plane wave impulse approximation (PWIA) [15] as:

$$\frac{d\sigma_{\mathrm{PWIA}}}{d\Omega}(E_\gamma,\Theta_\pi) = \frac{s}{m_N^2}A^2\frac{d\sigma_{NS}}{d\Omega}\left(E_\gamma^\star,\Theta_\pi^\star\right)F^2(q_A), \quad (1)$$

$$\frac{d\sigma_{NS}}{d\Omega}\left(E_\gamma^\star,\Theta_\pi^\star\right) = \frac{1}{2}\frac{q^\star}{k^\star}\left|\mathcal{F}_2\left(E_\gamma^\star,\Theta_\pi^\star\right)\right|^2\sin^2\left(\Theta_\pi^\star\right), \quad (2)$$

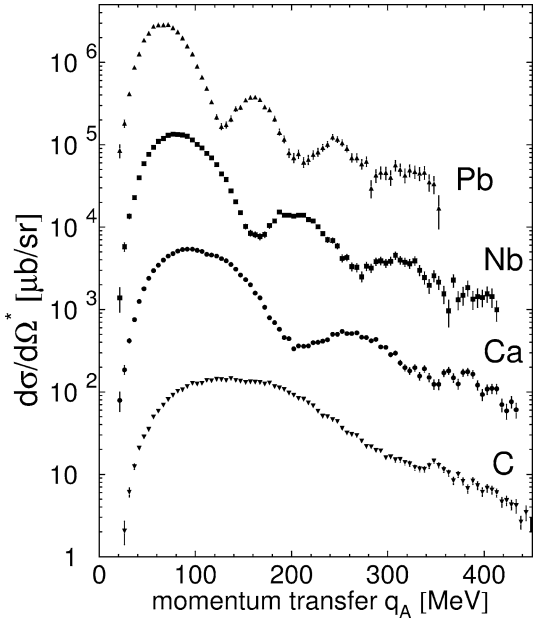

Fig. 2. Differential cross sections for $A(\gamma,\pi^0)A$ averaged over incident photon energies from 200–290 MeV as function of the momentum transfer. The scale corresponds to the carbon data, the Ca-, Nb- and Pb-data are scaled up by factors 10, 100, 1000, respectively.

where E_γ and Θ_π are the incident photon energy and the pion polar angle in the *photon–nucleus* cm-system, A is the atomic mass number, m_N is the nucleon mass and $F(q_A)$ the nuclear mass form factor The total energy $\sqrt{s}$ of the photon–nucleon pair, the photon energy and momentum $E^\star_\gamma$, $k^\star$, and the pion angle and momentum $\Theta^\star_\pi$, $q^\star$ in the *photon–nucleon* cm-system are evaluated from the average momentum $\vec{p}_N$ of the nucleon in the factorization approximation $\vec{p}_N = \vec{q}_A(A-1)/2A$. The spin-independent elementary cross section $d\sigma_{NS}/d\Omega$ is calculated from the standard Chew–Goldberger–Low–Nambu (CGLN) amplitude $\mathcal{F}_2$ [29] taken from [16] and averaged over proton and neutron numbers.

The influence of the form factor and the $\sin^2$-term, which forces the forward cross section to zero, is clearly visible in Fig. 2. The data allow also a direct check of the characteristic A^2-dependence. For this purpose we define the ratio:

$$R_{\mathrm{PWIA}} = \left(\frac{d\sigma_{\mathrm{exp}}}{d\Omega}\right) \Big/ \left[\frac{s}{m_N^2} A^2 \left(\frac{d\sigma_{NS}}{d\Omega}\right)\right] = F^2(q_A) \left(\frac{d\sigma_{\mathrm{exp}}}{d\Omega}\right) \Big/ \left(\frac{d\sigma_{\mathrm{PWIA}}}{d\Omega}\right) \qquad (3)$$

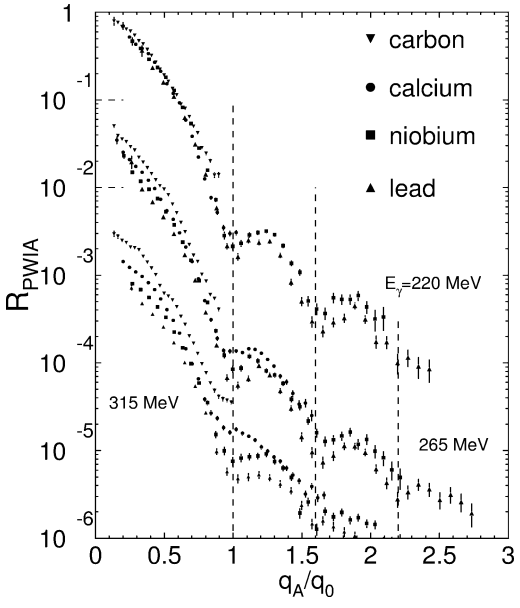

Fig. 3. Ratio R_{PWIA} (see Eq. (3)) as function of q_A/q_0 where q_0 is the momentum transfer at the first minimum of the form factor. The scale corresponds to the 220 MeV data, the 265, 315 MeV data are scaled down by factors 10, 100.

which is plotted in Fig. 3 versus q_A/q_0, where q_0 is the momentum transfer at the first diffraction minimum. As long as PWIA is valid, the ratios should equal the square of the nuclear mass form factors, which are similar for all nuclei as function of q_A/q_0. For the lowest incident photon energies around 220 MeV the ratios for all nuclei are indeed very similar and close to unity for small momentum transfers which demonstrates the approximate validity of the PWIA in this region. For higher photon energies we expect significant FSI effects since the pions then have a much larger cross section for the excitation of the Δ-resonance. The data show this effect as a decrease of the cross section ratio with mass number.

A detailed investigation of the FSI effects and possible medium modifications of the Δ-resonance requires an analysis far beyond PWIA. As a first step the angular distributions for ^{12}C, ^{40}Ca and Pb are compared in Fig. 4 to results from the model of Drechsel et al. [15]. The three curves in the figure correspond to PWIA, DWIA and the full model. In addition to pion FSI this includes also the medium modification of the Δ-resonance properties due to the Δ-nucleus interaction via a phenomenological parametrization of the Δ self-energy. The Δ self-energy was fitted to the $^4\mathrm{He}(\gamma,\pi^0)^4\mathrm{He}$ reaction [15,24] and this parametrization was used without modification to calculate the cross sections for C, Ca and Pb.

At low incident photon energies ($E_\gamma = 200$ MeV) the difference between PWIA, DWIA and additional Δ-modification is small. However, the cross sections are strongly overestimated around the Δ-resonance position by the PWIA and DWIA calculations. This in contrast to our results for coherent photoproduction from the deuteron [23] which are in good agreement with the DWIA calculation. Reasonable agreement for the heavier nuclei is only achieved when the Δ-nucleus interaction is taken into account. The Δ-self energy extracted from the ^{4}He data for this incident photon energy ($E_\gamma = 290$ MeV) is $\mathrm{Re}(V) \approx 19$ MeV and $\mathrm{Im}(V) \approx -33$ MeV [15], corresponding to a significant effective broadening of the resonance by 66 MeV. Based on a comparison of their prediction to the few data then available for $^{12}\mathrm{C}(\gamma,\pi^0)^{12}\mathrm{C}$ it was suggested by Drechsel et al. [15] that the Δ-nucleus interaction already saturates for ^{4}He. The present data demonstrate that indeed the A-dependence of the potential is not large since the agreement between model

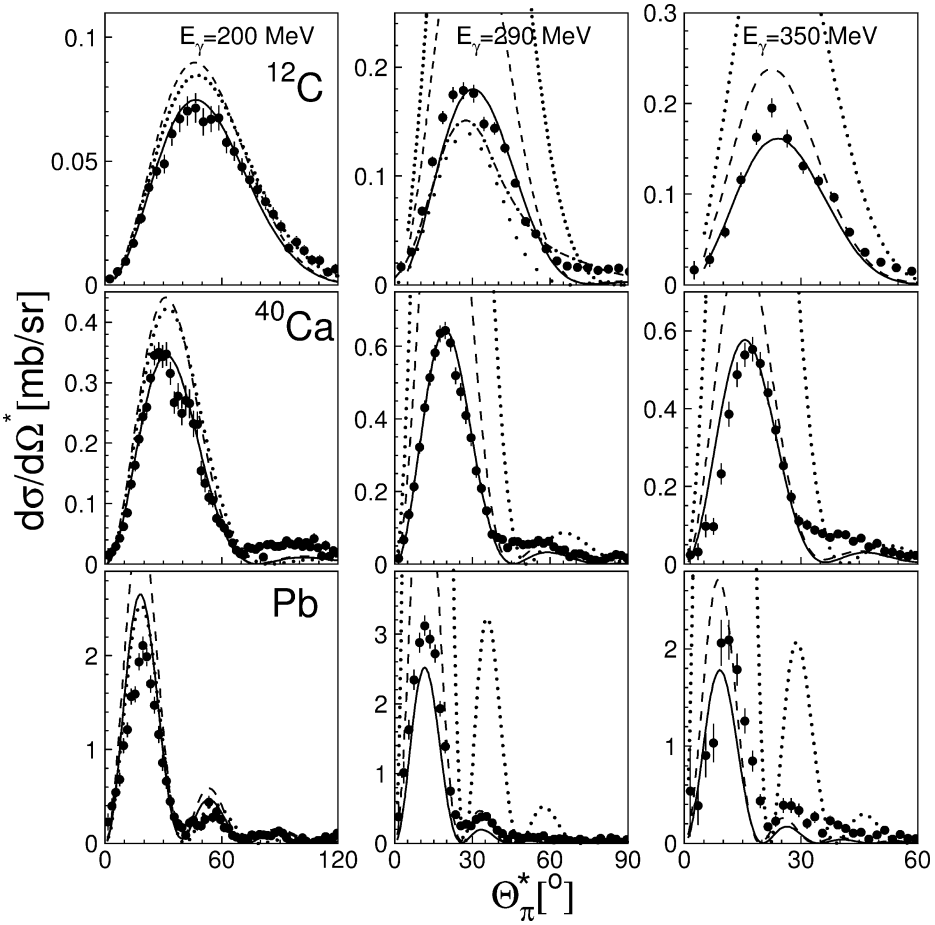

Fig. 4. Differential cross sections for $^{12}C(\gamma,\pi^0)^{12}C$, $^{40}Ca(\gamma,\pi^0)^{40}Ca$, and $Pb(\gamma,\pi^0)Pb$ compared to the predictions from Drechsel et al. [15]. Dotted lines: PWIA, dashed lines: DWIA, full lines: DWIA with Δ-self energy fitted to ^{4}He cross sections. For the carbon data at 290 MeV the predictions from Ref. [13] for the coherent reaction (wide space dotted) and coherent plus incoherent excitation of low lying states (dash-dotted) are also shown.

predictions and data is very good for carbon and calcium and still reasonable for lead.

A more detailed comparison of the data to model predictions requires some remarks concerning possible background from incoherent excitations of nuclear levels. It was pointed out by Takaki et al. [13] that such components will have a significant effect on the total cross section since they peak at more central pion angles which gives them a large weight for the total cross section. The prediction of the angular distribution for ^{12}C at $E_\gamma = 290$ MeV from their Δ-hole model with and without incoherent excitations is also compared to the data in Fig. 4. The model underestimates the data, even when incoherent excitations are included. Some examples of the differential cross sections weighted with $\sin(\Theta^\star_\pi)$ are compared to the predictions from [15] in Fig. 5. This presentation shows directly the contribution of different angular ranges to the total cross section. A first estimate of the total coherent cross sections has been obtained by integration of the angular distributions up to momentum transfers of 330, 340, 360 MeV for ^{12}C, ^{40}Ca, ^{93}Nb and Pb, respectively. These momentum transfers (see Fig. 2) correspond to the position of the first (C), second (Ca), third (Nb) and fourth (Pb) minimum of the form factor. The results of the integration are shown in Fig. 6. This

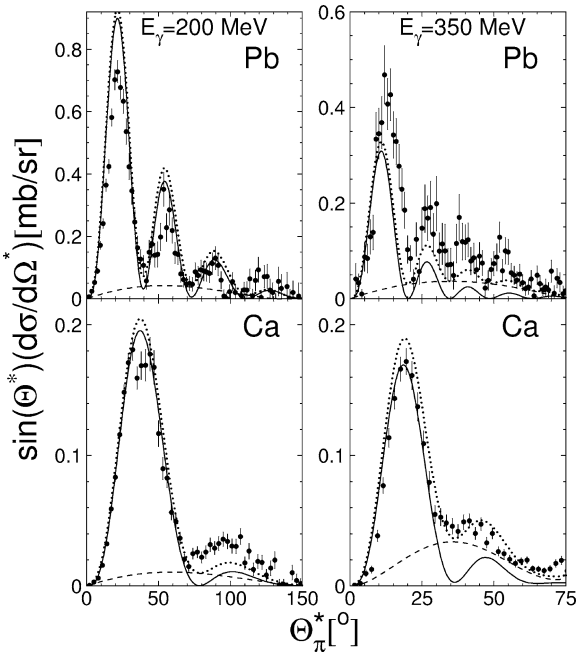

Fig. 5. Differential cross sections for ^{40}Ca$(\gamma,\pi^0)^{40}$Ca, and Pb(γ,π^0)Pb multiplied by sin$(\theta^\star)$. The full curves are the predictions from Drechsel et al. [15] for the coherent process. The dashed lines indicate the estimate (see text) for possible incoherent contaminations of the data. The dotted lines show the sum of the prediction for the coherent cross section and the incoherent background.

restriction of the angular ranges is reasonable since the model [15] predicts that approximately 98% of the total coherent cross section is contained in these ranges, but it significantly suppresses incoherent background which occurs at higher momentum transfers (as shown for ^{12}C in Fig. 6). Since the total cross sections obtained in this way (open circles in Fig. 6) may still include residual background from incoherent processes in the chosen angular ranges they represent only an *upper* limit of the coherent cross section. An estimate of these incoherent contributions has been obtained under the assumption that the differential cross section in the diffraction minima of the coherent process is entirely due to incoherent processes and that these contributions can be smoothly interpolated (see Fig. 5). The estimated corrections are in the range 12%–16% at $E_\gamma = 200$ MeV and 14%–26% at $E_\gamma = 350$ MeV. These corrections are certainly overestimates since the DWIA calculations from [15] indicate that the coherent cross section is not zero at the diffraction minima and this will be further accentuated by the experimental resolution. The corrected data (filled circles in Fig. 6) thus represent a *lower* limit of the coherent cross section. The results with this correction are compared to previous data and model predictions in Fig. 6. The only data available in this energy region so far are from the experiment of Arends et al. [22] who used an active target for the separation of coherent and non-coherent events in π^0-photoproduction from ^{12}C. However, in that experiment events from breakup reactions, e.g., with a low energy neutron in the final state could not be completely suppressed. The comparison to the new data shows that at higher energies such contaminations were obviously large. The model predictions by Drechsel et al. [15] are in good agreement with the carbon and calcium data but less so for lead. The local approximation to the Δ-hole model by Carrasco et al. [14] underestimates all total cross sections and shows a different energy dependence. The Δ-hole calculation for ^{12}C by Takaki et al. [13] also underestimates the data on an absolute scale, although the energy dependence is quite well reproduced. Note that in this case the data integrated over the full angular range (open diamonds in Fig. 6) represent a lower limit for the cross section of coherent plus incoherent events from [13] since part of the incoherent contribution in the data is suppressed by the missing energy cut. However, the prediction underestimates even this lower limit. Finally, the predictions from [18] for ^{40}Ca with vector and tensor parametrization of the elementary amplitude both disagree with the data.

4. Conclusion

Coherent π^0-photoproduction from nuclei was studied in detail throughout the Δ-resonance region. The characteristic features of the coherent process, the proportionality of the cross section to $\sin^2(\Theta_\pi)$, to the nuclear mass form factor and to the square of the nuclear mass numbers are demonstrated. The data are quite well reproduced by simple PWIA calculations at incident photon energies around 200 MeV, but at higher photon energies distortion effects become large. Predictions for the coherent cross section are available from many detailed theoretical studies, however the results from different models are not at all

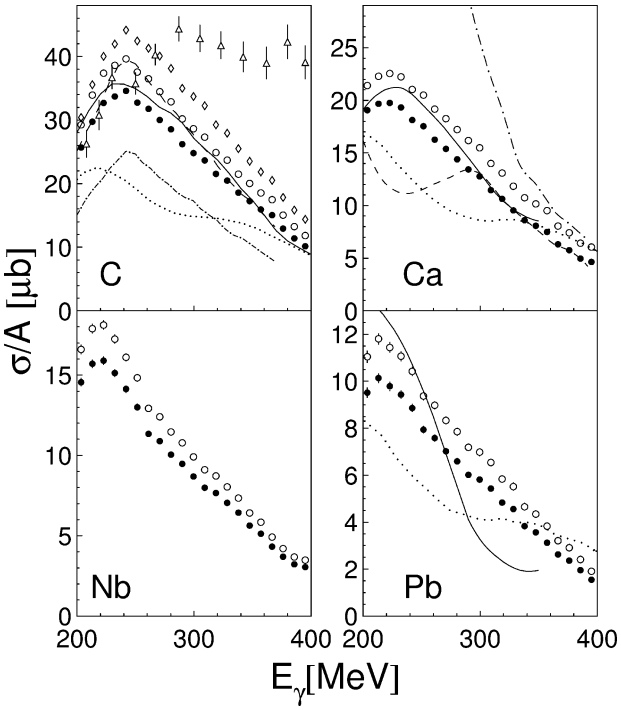

Fig. 6. Total cross sections for $^{12}C(\gamma,\pi^0)^{12}C$, $^{40}Ca(\gamma,\pi^0)^{40}Ca$, and $Pb(\gamma,\pi^0)Pb$. Open circles: cross section obtained by integration of the differential cross sections up to momentum transfers of 330 MeV (carbon), 340 MeV (calcium) and 360 MeV (niobium, lead). Filled circles: with correction for incoherent contamination (see text). Full curves: prediction by Drechsel et al. [15]. The dotted lines are predictions from Carrasco et al. [14]. For carbon the open diamonds show the total cross section by integration over the full angular range, the open triangles are data from Ref. [22]. The dash-dotted and dashed curves are the prediction from [13] for the coherent and coherent plus incoherent processes, respectively. For calcium the dashed and dash-dotted lines are the predictions from Ref. [18] for vector (dashed) and tensor (dash-dotted) parametrization of the elementary amplitude.

in agreement (see Fig. 6). Best agreement with the data is found for the model by Drechsel et al. [15]. A comparison of the experimental results to these calculations demonstrates their sensitivity to medium modifications of the Δ-isobar. It is shown, that reasonable agreement between data and model predictions for all nuclei is achieved with a parametrization of the Δ-self energy fitted to the differential cross sections of the reaction $^4He(\gamma,\pi^0)^4He$. This is an indication that the Δ-nucleus potential is not strongly dependent on the nuclear mass number but saturates already for ^4He.

Acknowledgements

We wish to acknowledge the outstanding support of the accelerator group of MAMI, as well as many other scientists and technicians of the Institute für Kernphysik at the University of Mainz. We thank M. Röbig-Landau for his contribution to the calibration and analysis of the data. We gratefully acknowledge many stimulating discussions with L. Tiator. This work was supported by Deutsche Forschungsgemeinschaft (SFB 201) and the UK Science and Engineering Research Council.

References

[1] J. Lehr, M. Effenberger, U. Mosel, Nucl. Phys. A 671 (2000) 503.
[2] R.C. Carrasco, Phys. Rev. C 48 (1993) 2333.
[3] M. Röbig-Landau et al., Phys. Lett. B 373 (1996) 45.
[4] B. Krusche et al., Phys. Rev. Lett. 86 (2001) 4764.
[5] C. Caso et al., Review of Particle Properties, Eur. Phys. J. C 3 (1998) 1.

[6] V. Girijia et al., Phys. Rev. C 27 (1983) 1169.
[7] S.S. Kamalov et al., Phys. Lett. B 162 (1985) 260.
[8] S. Boffi et al., Nucl. Phys. A 448 (1986) 637;
S. Boffi et al., Nuovo Cimento A 104 (1991) 843.
[9] A.A. Chumbalov et al., Z. Phys. A 328 (1987) 195;
A.A. Chumbalov et al., Phys. Lett. B 196 (1987) 23.
[10] E. Oset, W. Weise, Nucl. Phys. A 402 (1983) 612.
[11] J.H. Koch, E.J. Moniz, Phys. Rev. C 27 (1983) 751.
[12] B. Körfgen et al., Phys. Rev. C 50 (1994) 1637.
[13] T. Takaki et al., Nucl. Phys. A 443 (1985) 570.
[14] R.C. Carrasco et al., Nucl. Phys. A 565 (1993) 797.
[15] D. Drechsel et al., Nucl. Phys. A 660 (1999) 423.
[16] D. Drechsel et al., Nucl. Phys. A 645 (1999) 145;
D. Drechsel et al., http://www.kph.uni-mainz.de/MAID/maid.html.
[17] W. Peters, H. Lenske, U. Mosel, Nucl. Phys. A 640 (1998) 89.
[18] L. Abu Raddad et al., Phys. Rev. C (1999) 054606.
[19] R.A. Schrack et al., Phys. Rev. 127 (1962) 1772;
R.A. Schrack et al., Phys. Rev. B 140 (1965) 897.
[20] R.W. Gothe et al., Phys. Lett. B 355 (1995) 59.
[21] G. Koch et al., Phys. Rev. Lett. 63 (1989) 498;
G. Koch et al., Phys. Lett. B 218 (1989) 143.
[22] J. Arends et al., Z. Phys. A 311 (1983) 367.
[23] B. Krusche et al., Eur. Phys. J. A 6 (1999) 309.
[24] F. Rambo et al., Nucl. Phys. A 660 (2000) 69.
[25] V. Bellini et al., Nucl. Phys. A 646 (1999) 55.
[26] D.R. Tieger et al., Phys. Rev. Lett. (1984) 755.
[27] R. Novotny, IEEE Trans. Nucl. Sci. 38 (1991) 379.
[28] A.R. Gabler et al., Nucl. Instrum. Methods A 346 (1994).
[29] G.F. Chew et al., Phys. Rev. 106 (1957) 1345.